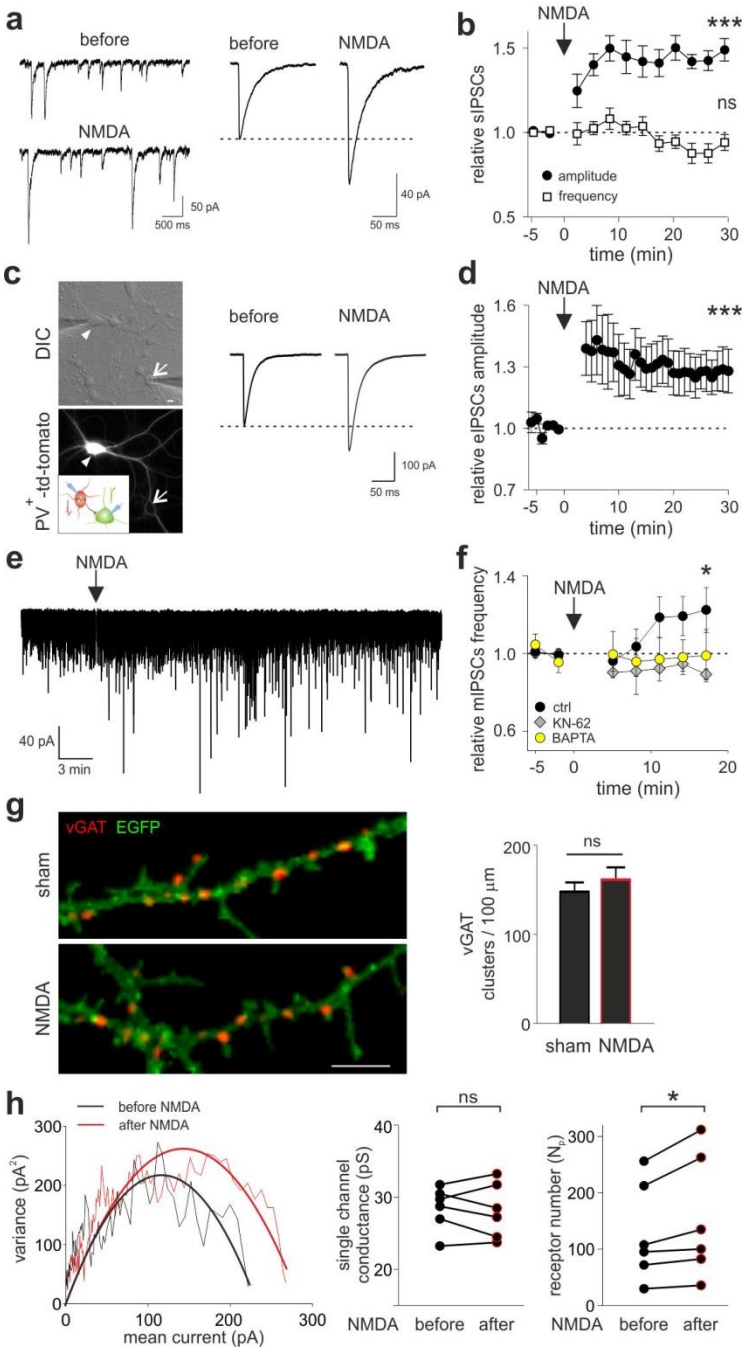

Supplementary Fig. 1. Supplementary data on NMDA-induced potentiation of inhibition

(**a**) Left: Example traces of sIPSCs recordings before and after NMDA treatment showing an increase of current amplitude that lasts up to 30 min. Right: Representative sIPSCs traces averaged from 20 events recorded from the same neuron before and 20 minutes after NMDA

treatment. (**b**) Time course of relative sIPSCs amplitude and frequency increase after NMDA application (plain arrow). (**c**) Top: DIC image showing two patched neurons in the paired-patch configuration (arrow, postsynaptic and arrowhead, presynaptic). Bottom: Fluorescence image showing that the presynaptic neuron is a parvalbumin-positive (PV+) td-tomato expressing interneuron. Inset: schematization of the experimental approach: an action potential is evoked from the presynaptic PV+ interneuron and the elicited GABAergic current is recorded from the postystynaptic neuron. Right: Representative eIPSCs traces averaged from 20 events elicited in the same postsynaptic neuron before and 20 minutes after NMDA treatment. (**d**) Time course of relative eIPSCs amplitude increase after NMDA application (plain arrow). (**e**) Example trace of a mIPSCs recording before and after NMDA treatment (plain arrow) showing an increase of current amplitude that lasts up to 30 min. (**f**) Time course of relative mIPSCs frequency after NMDA application (plain arrow) in control and upon KN-62 or intracellular BAPTA application. (n=12-18) (**g**) Left: Representative confocal images of GABAergic synapses (vGAT, red), impinging on an EGFP-transfected cultured hippocampal neuron treated with sham solution or NMDA. Scalebar, 5μm. Right: Quantification of vGAT cluster density in sham- and NMDA-treated neurons. n = 24 cells from 3 independent preparations. (**h**) Peak-scaled non stationary analysis performed under control conditions and after iLTP. Left: Parabolic mean-variance relationship under control conditions before and after iLTP induction. Middle, right: Mean single channel conductance values and number of channels open at the current peak (N_p) (right) obtained before and after iLTP induction by fitting the mean-variance relationships with the formula $\sigma^2 = iI - I^2/N_p$ (see methods) (n=6, p=0.03, paired t-test). Error bars represent sem. $p<0.05$; ***$p<0.001$.

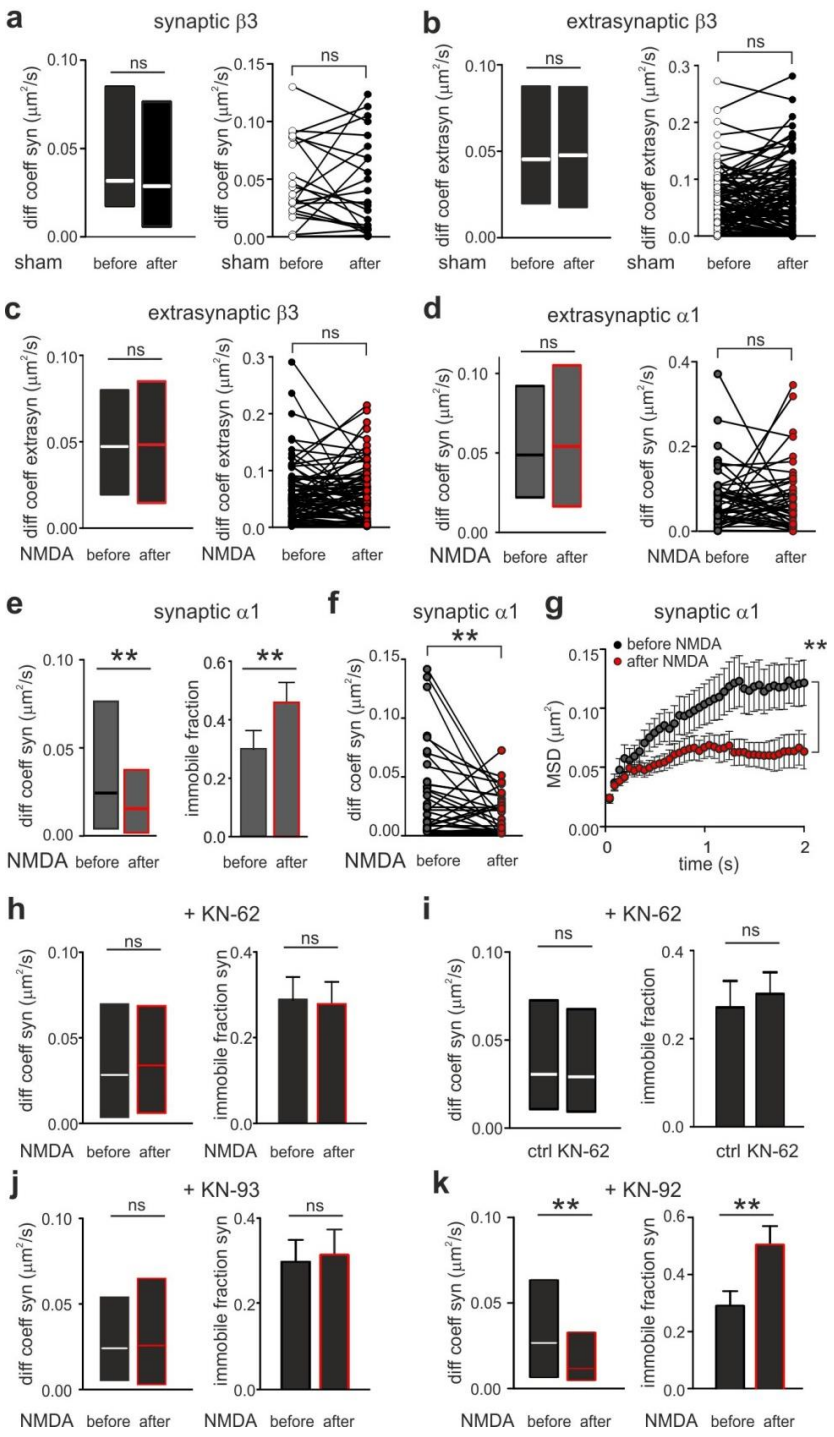

Supplementary Fig. 2. Control experiments for the SPT results reported in Fig. 1

(**a**) Median ± IQR diffusion coefficient (left: all, n= 93; right: matched values, n = 24) of synaptic β3 receptors before and after application of sham solution. (**b**) Diffusion coefficient of

extrasynaptic β3 receptors before and after application of sham solution (left: all, n= 194-200; right: matched values, n= 125). (**c**) Comparable diffusion coefficient (median ± IQR) (left: all, n= 232-241 and right: matched values, n= 83) of extrasynaptic β3 receptors before and after NMDA treatment. (**d**) The mobility of extrasynaptic α1 receptors is not affected by NMDA stimulation (similarly to recombinant β3 receptors, see panel b). $n_{trajectories}$ total= 122 and matched= 52. (**e**) Median ± IQR diffusion coefficient (left) and immobile fraction (right) of endogenous α1 subunit-QD complexes at GABAergic synapses before and after NMDA stimulation. $n_{trajectories}$ = 72. (**f,g**) Matched diffusion coefficient (**f**) and MSD over time (**g**) values of individual endogenous $GABA_A$Rs observed at synapses before and after NMDA treatment. $n_{trajectories}$ = 36. (**h**) Median diffusion coefficient and IQR of all synaptic β3 receptors in the visual field in the presence of KN-62 before NMDA ($n_{trajectories}$=211) after NMDA ($n_{trajectories}$=202; p>0.05, Mann-Whitney U-test) and the corresponding immobile fraction (n=202-211; p>0.05, Student's t-test). (**i**) Left: Diffusion coefficient (median ± IQR) of total $GABA_A$R at synapses in untreated (control) and KN-62 treated neurons. Right: Fraction of immobile $GABA_A$R at synapses in control conditions and after treatment with KN-62 (right). n= 86-107. (**j,k**) Median diffusion coefficient (left) and immobile fraction (right) of total synaptic β3 receptors before and after NMDA stimulation upon treatment with KN-93 (**j**) or KN-92 (**k**). Unless otherwise stated, data are expressed as means ± sem. **, p<0.01; ns, non-significant.

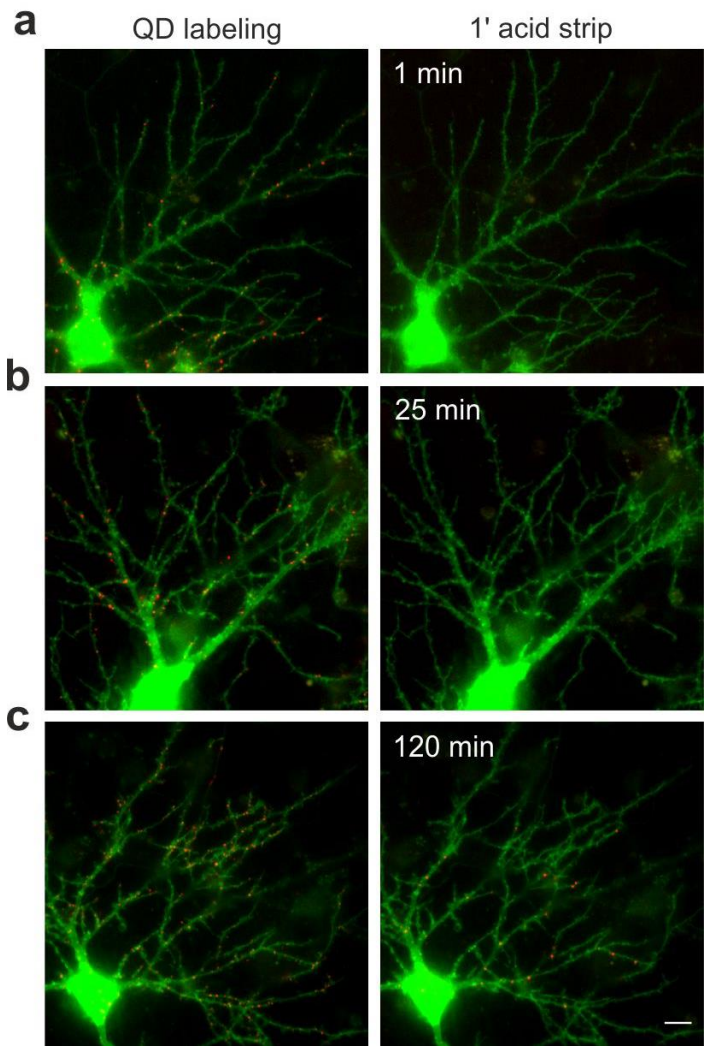

Supplementary Fig. 3. QD-receptor complexes are not internalized during the chem-iLTP experiment duration

(**a,b,c**) Left: representative images showing conventional surface $GABA_ARs$ labeling with QDs (red) in GFP-expressing neurons (green). Right: Residual QDs detected after acid strip (1 min) performed 1, 25 or 120 min (**a,b,c**, respectively) after the initial labeling. The presence of residual QDs when the acid strip is performed 120 min post labeling (panel c), a time duration compatible with receptor endocytosis, shows that internalized QDs can be detected (positive control). The lack of QDs in panel a (acid strip 1 min after labeling) indicates that the acid wash

efficiently removes surface QD-antibody complexes (negative control). The absence of QDs when the acid strip is performed 25 min after the labeling, i.e. at the end of the chem-LTP experiments, indicates that, over the SPT experiments duration, only surface $GABA_AR$s are tracked, being QD-receptors internalization minimal.

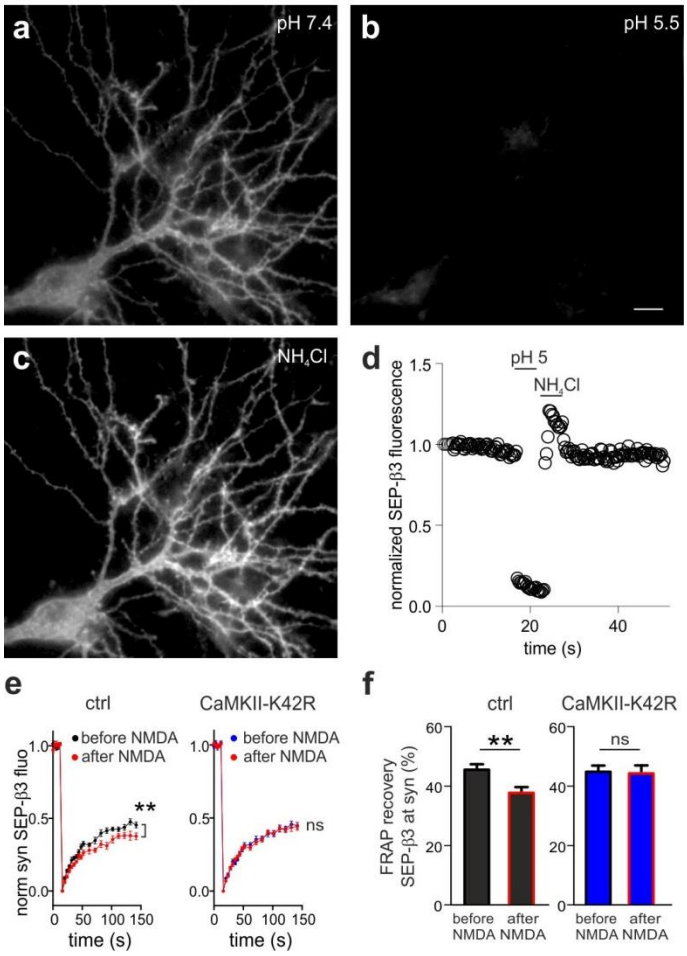

Supplementary Fig. 4. Probing total surface $GABA_ARs$ lateral mobility by fluorescence recovery after photobleaching

(**a-d**) The pH sensitivity of SEP-β3 demonstrates that only surface receptors emit fluorescence. (**a-c**) Representative images of a DIV 16 cultured hippocampal neuron transfected with SEP-β3 (at DIV 7) subsequently exposed to: (**a**) a pH 7.4 solution; (**b**) pH 5 solution; (**c**) NH_4Cl solution. The disappearance of SEP signal upon perfusion of the neuron with an acidic solution indicates that only surface receptors emit fluorescence. The fluorescence increase (as compared to pH 7.4) induced by NH_4Cl due to collapse of intracellular pH gradients shows that SEP-β3 is quenched in intracellular acidic compartments. (**d**) Quantification of the relative changes of SEP-β3

fluorescence of the neuron in (a-c) over time upon perfusion with a pH 7.4, pH 5 and NH_4Cl solutions. (**e,f**) Probing the mobility of total surface β3 subunit-containing receptors during chem-iLTP by fluorescence recovery after photobleaching of SEP-β3. (**e**) Average normalized fluorescence over time of SEP-β3 in bleached synaptic areas observed in the same cell before and after NMDA treatment in control (mCherry) and in CaMKII-K42R-mCherry-expressing neuronal cultures. Receptor mobility is expressed as fluorescence recovery after photobleaching (FRAP) in the bleached area, normalized to the fluorescence before bleaching and setting to zero the residual fluorescence at the time of the bleaching. (**f**) Quantification of the FRAP recovery (150 sec after bleaching) of synaptic $GABA_A$Rs before and after NMDA in control neurons (before: 45.4±1.8 %; NMDA: 37.6±1.9 %; p=0.008, Student's t test) and in CaMKII-K42R-expressing neurons (before: 44.8±2.1%; NMDA: 44.2±2.6; p>0.05, Student's t test). Error bars represent sem. *, p>0.05; **, p<0.01 and ns, non significant.

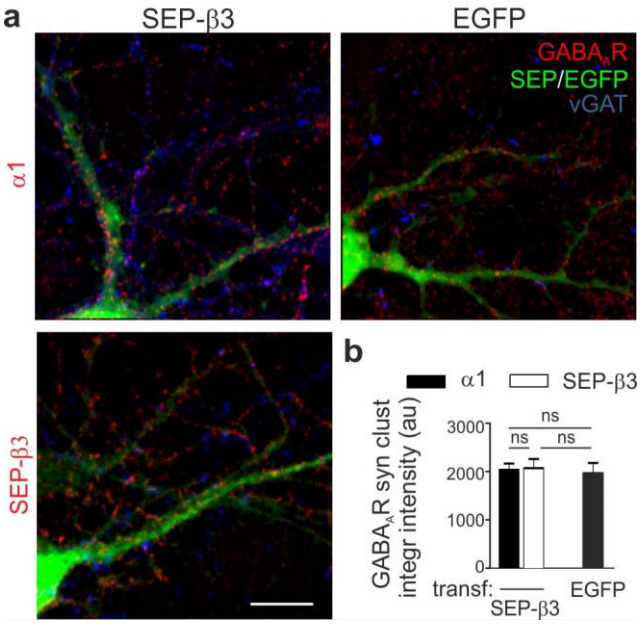

Supplementary Fig. 5. Reliability of immunocytochemical experiments on neurons overexpressing recombinant GABA$_A$R subunits as compared to the endogenously expressed subunits.

(**a**) Confocal images examples of neurons transfected with SEP-β3 and immunolabeled (red) for α1 or SEP (to probe recombinant β3 subunit) show that GABA$_A$R cluster intensity is similar to that in control neurons transfected with EGFP and immunoprobed for endogenous α1. (**b**) Quantification of the experiment described in A. N = 24 cells from 3 independent preparations in each condition. Scalebar, 10 μm. Error bars represent sem. ns, non significant.

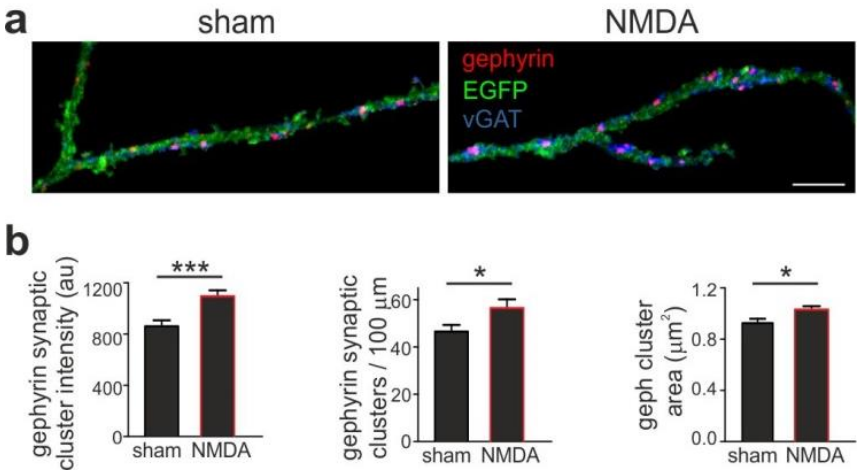

Supplementary Fig. 6. NMDA-induced increase of synaptic gephyrin detected with an alternative anti-gephyrin antibody

(**a**) Confocal images examples of gephyrin clusters (red) accumulation at synapses (vGAT, blue) in hippocampal neurons transfected with EGFP (green) after sham or NMDA treatment. Gephyrin was detected with the mAb3B11 antibody. Note that these results are comparable with those obtained by using the mAb7a anti-gephyrin antibody (Fig. 4a,b). (**b**) Quantification of the integrated intensity, the density and the area of gephyrin synaptic clusters. n=25 in each condition; *, $p<0.05$; ***, $p<0.001$; Student's t-test.

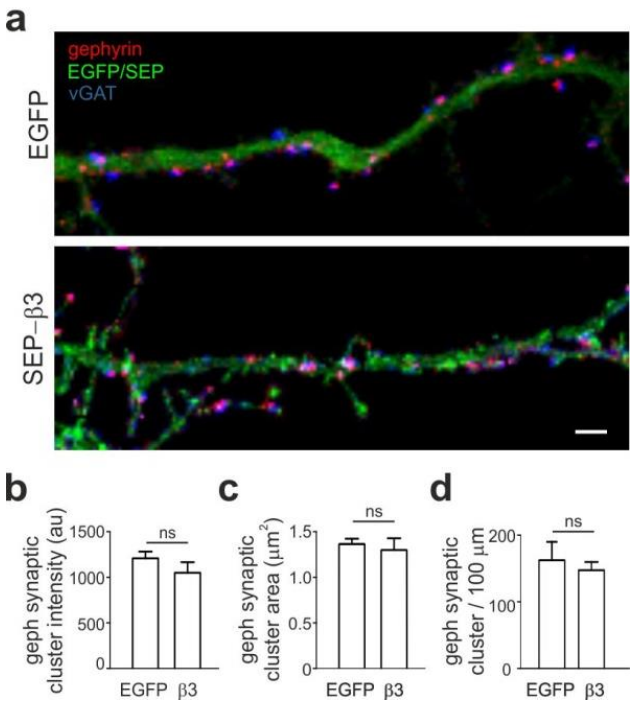

Supplementary Fig. 7. Gephyrin availability is comparable in EGFP- and β3-expressing neurons.

(**a**) Confocal images examples of neurons transfected with either EGFP or SEP-β3 and immunoprobed for gephyrin (red) and vGAT (blue). Colocalization or partial overlap of gephyrin and vGAT fluorescence signals is reported in pink. Scalebar, 10 μm. (**b-d**). Quantification of the integrated intensity (**b**), area (**c**) and density (**d**) of gephyrin synaptic clusters. n = 24 cells in each condition, from 3 independent preparations. Data are expressed as mean ± sem. ns, non significant.

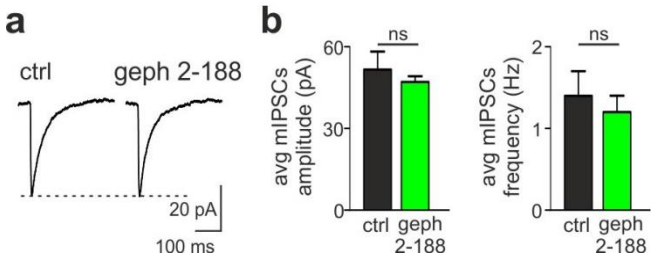

Supplementary Fig. 8. GABAergic mIPSCs are not affected by impairment of gephyrin assembly

(**a**) Representative average mIPSCs traces recorded from control and gephyrin 2-188-expressing neurons in basal conditions. (**b**) Bar plots of average mIPSCs amplitude and frequency in control (n=12) and 2-188-expressing neurons (n=12, Student's t-test). Data are expressed as means ± sem. ns, non significant.

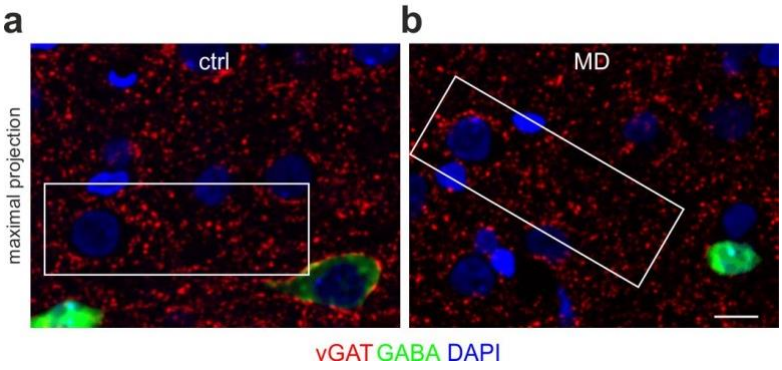

Supplementary Fig. 9. Complementary images of four-color immunohistochemistry probing $GABA_A$Rs, vGAT, GABA and DAPI in MD and control animals

(**a,b**) Representative maximal projections of 18 confocal z-stack (7.5 μm depth) confocal images of cortical slices from control (a) and MD animals (b) associated with those shown in Fig. 10. Inhibitory synapses immunoprobed with vGAT are represented in red, GABA-positive inhibitory neurons (excluded from the analysis) are shown in green and DAPI is in blue. Scalebar, 10 μm. Since the simultaneous visual representation of four-colors immunohistochemistry (where also $GABA_A$Rs are immunolabeled) would be difficult to decipher, for sake of clarity, Fig. 10 a,b and Supplementary Fig. 9a,b show $GABA_A$Rs/vGAT/DAPI and vGAT/DAPI and GABA, respectively.

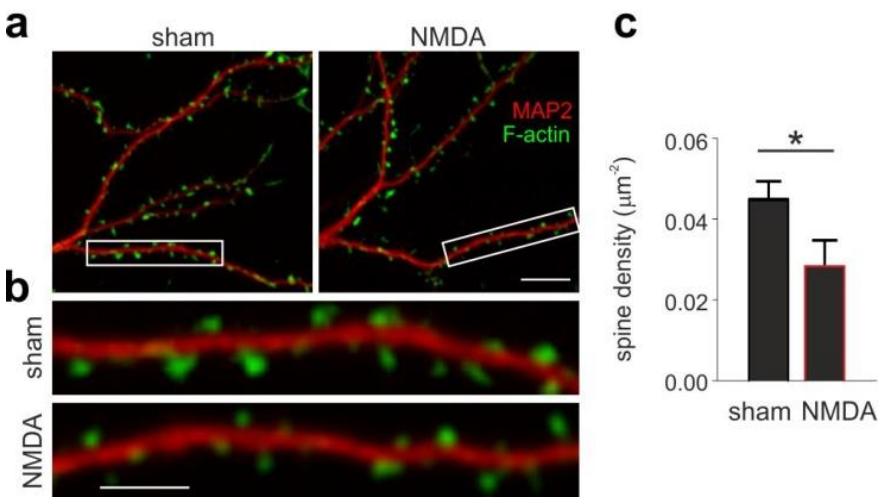

Supplementary Fig. 10. Besides chem-iLTP, NMDA stimulation concomitantly induces LTD at glutamatergic synapses with spine loss

(**a**) Example images of F-actin (stained with phalloidin-Alexa 546, green) and MAP2 (red) in neurons treated with sham or NMDA solutions. Scalebar 10 μm. (**b**) Magnification of the boxes framed above, showing spines on a dendrite form sham- (top) or NMDA- (bottom) treated neuron. Scalebar 5 μm. (**c**) Quantification of spine density (expressed as spines per μm^2) in sham- and NMDA-treated neurons (n = 24 cells from 3 independent preparations). Error bars represent sem. ns, non significant. p=0.03, Student's t-test.

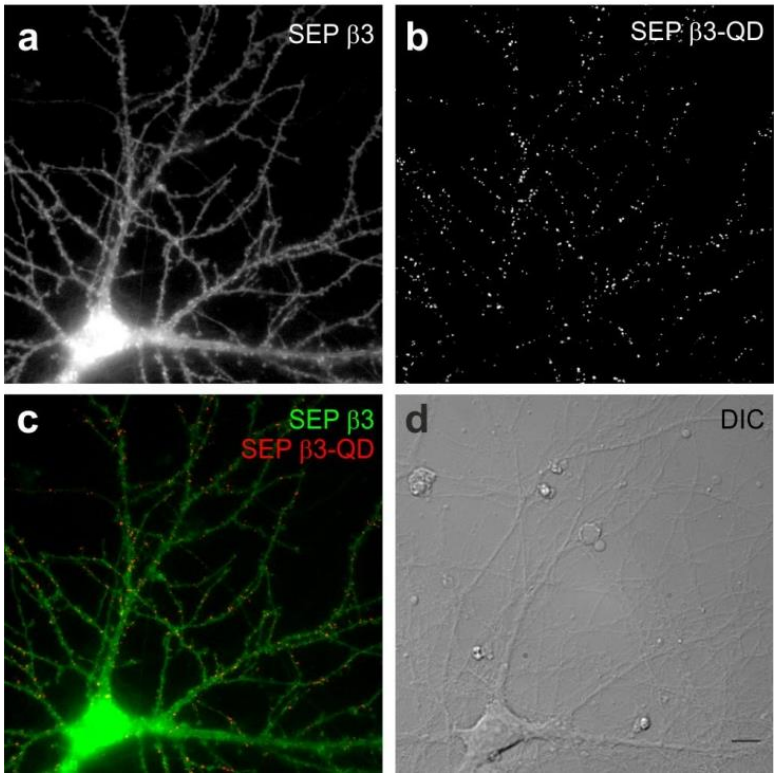

Supplementary Fig. 11. Specificity of QD labeling

Representative images of a neuron transfected with SEP-β3 (**a**) and labeled with anti GFP-coupled QDs (**b**). Since SEP is a modified version of GFP, the anti GFP antibody recognizes the SEP tag on the β3 subunit. (**c**) Merge of the micrographs in panel (a) and (b), showing overexpressed SEP-β3 in green and QDs in red. (**d**) Differential interference contrast (DIC) image showing the neuron in panels a-c and neighboring untransfected neurons. The exclusive presence of QDs over the signal of the transfected neuron and the absence of QDs on untransfected neurons demonstrate the selectivity of QD labeling. Scalebar, 10 μm.